Revised vertical cloud structure of Uranus from UKIRT/UIST observations and changes seen during Uranus' Northern Spring Equinox from 2006 to 2008: Application of new methane absorption data and comparison with Neptune

P.G.J. Irwin[*], N.A. Teanby[*], and G.R. Davis[†]

[*]Atmospheric, Oceanic, and Planetary Physics, Department of Physics, University of Oxford, Clarendon Laboratory, Parks Rd, Oxford, OX1 3PU, United Kingdom

Tel: (+44) 1865 272933, *Fax:* (+44) 1865 272923.

E-mail: irwin@atm.ox.ac.uk

[†]Joint Astronomy Centre, 660 N. A'ohoku Place, Hilo, Hawaii 96720

Original: September 29th 2009

Revised: March 11th 2010

Number of manuscript pages: 24 + acknowledgements, references, and figure legends (50 in total)

Number of Figures: 17

Number of Tables: 2

Proposed running head:

Uranus' revised cloud changes through 2007 equinox

Editorial correspondence should be directed to:

Dr Patrick G. J. Irwin,

Atmospheric, Oceanic and Planetary Physics, Clarendon Laboratory, Parks Rd,

Oxford OX1 3PU, United Kingdom.

Telephone: (+44) 1865 272933 (direct line: 272083)

Fax: (+44) 1865 272923

Email: irwin@atm.ox.ac.uk

Abstract

Long-slit spectroscopy observations of Uranus by the United Kingdom Infrared Telescope UIST instrument in 2006, 2007 and 2008 have been used to monitor the change in Uranus' vertical and latitudinal cloud structure through the planet's northern spring equinox in December 2007.

These spectra were analysed and presented by Irwin et al. (2009), but since publication, a new set of methane absorption data has become available (Karkoschka and Tomasko, 2009b), which appears to be more reliable at the cold temperatures and high pressures of Uranus' deep atmosphere. We have fitted k-coefficients to these new methane absorption data and we find that although the latitudinal variation and inter-annual changes reported by Irwin et al. (2009) stand, the new k-data place the main cloud deck at lower pressures (2-3 bars) than derived previously in the H-band of ~3-4 bars and ~3 bars compared with ~6 bars in the J-band. Indeed, we find that using the new k-data it is possible to reproduce satisfactorily the entire observed centre-of-disc Uranus spectrum from 1-1.75 μm with a single cloud at 2-3 bars provided that we make the particles more back-scattering at wavelengths less than 1.2 μm by, for example, increasing the assumed single scattering albedo from 0.75 (assumed in the J and H bands) to near 1.0. In addition, we find that using a deep methane mole fraction of 4% in combination with the associated warm 'F' temperature profile of Lindal et al. (1987), the retrieved cloud deck using the new Karkoschka and Tomasko (2009b) methane absorption data moves to between 1 and 2 bars.

The same methane absorption data and retrieval algorithm were applied to observations of Neptune made during the same programme and we find that we can again fit the entire 1-1.75 μm centre-of-disc spectrum with a single cloud model,

providing that we make the stratospheric haze particles (of much greater opacity than for Uranus) conservatively scattering (i.e. $\omega=1$) and we also make the deeper cloud particles, again at around the 2 bar level more reflective for wavelengths less than 1.2 μm. Hence, apart from the increased opacity of stratospheric hazes in Neptune's atmosphere, the deeper cloud structure and cloud composition of Uranus and Neptune would appear to be very similar.

Keywords: SPECTROSCOPY; URANUS, ATMOSPHERE; NEPTUNE, ATMOSPHERE; INFRARED OBSERVATIONS

1. Introduction

Observations of the near-infrared spectrum of Uranus, made with the United Kingdom InfraRed Telescope (UKIRT), were used by Irwin et al. (2009) to determine the latitudinal-vertical cloud structure of Uranus and its variation through Uranus' northern spring equinox in 2008. Considerable differences were found between the retrievals conducted in the H-band (1.6 μm) and Long J (1.3 μm) reflectance peaks, which were attributed to different particle sizes at different altitudes. The unacceptably poor fit to the Short J (1.1 μm) spectral peak was interpreted as being due to errors in the extrapolation of the Irwin et al. (2006) methane k-coefficients to the very long cold paths found in Uranus' atmosphere at pressures greater than 1 bar and it was conceded that such errors (although less severe) might exist also in the Long J and H-band observations, making such inter-comparisons ambiguous.

Since the publication of our previous analysis, a major reworking of the available sources of near-infrared methane opacity has been made by Karkoschka and Tomasko (2009b), who suggest that the original methane dataset used (Irwin et al. 2006) is unreliable at pressures greater than ~1 bar in Uranus' cold atmosphere. A new set of methane band data has been provided by these authors, and these band data have here been fitted with k-coefficients and used to reanalyse our UKIRT observations of Uranus' near-infrared spectrum. We find that the retrievals in different spectral bands are much more consistent with each other using the new methane coefficients, allowing a much more reliable estimate to be made of particle sizes and back-scattering efficiencies.

2. Observations, data reduction and retrievals

As described by Irwin et al. (2009), observations were made with the 3.8-m United Kingdom InfraRed Telescope (UKIRT) using the UKIRT Imager Spectrometer (UIST) instrument in long-slit spectroscopy mode with the entrance slit, of width 0.48", aligned with Uranus' central meridian (Table 1). These data were reduced using the UKIRT facility software and then analysed using the NEMESIS retrieval model (Irwin et al., 2008), The main gaseous absorption in Uranus' near-IR spectrum is due to methane, for which the available line data in databases such as HITRAN and GEISA at wavelengths less than 2 μm are relatively sparse. The methane *k*-coefficients of Irwin et al. (2006) used in our last study have been reanalysed by Karkoschka and Tomasko (2009b) in conjunction with all other available sources of near-infrared methane absorption data and also with respect to Huygens/DISR descent data through Titan's atmosphere. Karkoschka and Tomasko (2009b) find that the methane *k*-coefficients of Irwin et al. (2006) extrapolate poorly at pressures greater than 1 bar in Uranus' atmosphere. Instead they have prepared a new set of band coefficients based on the Irwin et al. (2006) data, but revised to make them more consistent with other sources of data. We have fitted *k*-coefficients to these band data using the method of Irwin et al. (1996) and in this paper compare calculations made with these new *k*-data with those made using the previous absorption coefficients of Irwin et al. (2006). The only other gaseous absorber at these wavelengths is continuum induced absorption of H_2-H_2 and H_2-He, which was again modelled after Borysow (1991, 1992) and Zheng and Borysow (1995); an equilibrium ortho/para H_2-ratio was assumed at all altitudes and latitudes (Conrath et al., 1998; Fouchet et al., 2003).

[Table 1]

Since the size distribution and refractive indices of the aerosols in Uranus' atmosphere are not well known we again first attempted to retrieve the cloud structure independently from wavelength bands centred on each of the three main peaks: Short J (1.07 μm), Long J (1.28 μm), and H (1.57 μm), using an assumed set of particle properties. The wavelength range covered by each band was chosen to be small enough that variations in the particle scattering properties across the range were negligible, but large enough that they covered a sufficiently wide range of methane absorption coefficients to sound the aerosol opacity from low to high pressures. For the aerosol optical properties we calculated the variation of extinction cross-section with wavelength (using Mie theory), assuming a modified-gamma distribution of spherical particles of refractive index 1.4+0*i* with mean radius 1 μm and variance 0.05. This choice of the size distribution was based on the typical size distribution of particles found in giant planet tropospheres (Irwin et al. 1998) and previous studies of clouds in Uranus' atmosphere (Rages et al. 1991), while the choice of refractive index was arbitrary given that the composition of the particles in the main cloud deck is unknown, although for reference Satorre et al. (2008) and Brunetto et al. (2008) find that the refractive index of methane ice at very cold temperatures is ~1.3, and the refractive index of ammonia ice is ~1.4 (Martonchik et al. 1984). However, both choices have little effect on our retrievals other than to set the rate at which the extinction cross-section falls with increasing wavelength from reflectance peak to reflectance peak as can be seen in Fig. 1, where the effect of modifying a number of scattering parameters is presented. The single-scattering albedo of the particles was set to be 0.75, which was suggested to be suitable at these wavelengths (1.2 – 1.6 μm) from Keck Telescope Uranus observations by Sromovsky and Fry (2007), although these authors stress that this is not firm estimate. Similarly, the particle phase function

was set to that preferred by Sromovsky and Fry (2007), namely a single Henyey-Greenstein function with asymmetry parameter $g = 0.7$. As can be seen from Fig. 1, varying either parameter has an almost identical effect on the calculated spectrum. In addition to scattering by these cloud particles, Rayleigh scattering from the air molecules themselves was also included. The importance of this may also be gauged from Fig. 1, where it can be seen that a purely Rayleigh scattering atmosphere with no additional aerosols provides a reasonably close approximation to the observed Uranus spectrum between reflectance peaks, pointing to the known very low opacity of stratospheric hazes in Uranus' atmosphere (e.g. West et al., 1991). The effect of varying the assumed particle size is also shown in Fig. 1, where we can see that reducing the mean radius leads to enhanced reflection in the shortwave peaks.

[Figure 1]

The near-IR spectrum of Uranus depends upon the vertical distribution of aerosols and methane, whose abundance is itself dependent on the vertical temperature profile since methane condenses in Uranus' cold atmosphere. For this study our temperature profile was based on the 'D' profile determined by radio-occultation from Voyager 2 by Lindal et al. (1987) and extended to higher pressures in the troposphere assuming a saturated adiabatic lapse rate. Although the Lindal 'D' profile is based on only a few measurements near to Uranus' southern solstice, very little latitudinal variation of temperature is expected on the giant planets at pressures greater than 1 bar and thus the assumed temperature profile was fixed for these retrievals and used at all latitudes.

Previous studies have reported a range of estimates on the abundance profile of methane in Uranus' atmosphere. Recently, Karkoschka and Tomasko (2009a) have used HST STIS observations to estimate the deep mole fraction of methane to be

roughly 4% at latitudes equatorwards of 45°, reducing to 1-2% polewards of 45°. Such an observation would be consistent with observations by the VLA from 1-6 cm (Orton et al., 2007), which show considerably more emission polewards of 45° N, S. These wavelengths are sensitive to emission from the 1-50 bar range and given, as mentioned before, that it is unlikely that temperatures are varying with latitude at such pressures, it suggests a considerable difference in the abundance of absorbers such as ammonia and methane. For this paper, where we compare the retrieved cloud structure using different methane absorption data and with previous work, we chose initially to keep the methane profile fixed at all latitudes with a deep methane mole fraction q_{CH4} of 1.6% relative humidity of 30%. The effect of increasing the methane abundance at some latitudes is investigated later.

Fits to the H-band (1.57 μm) reflectance peak

As in our previous analysis (Irwin et al., 2009) the measured spectra across Uranus' disc in the 1.57 μm peak were again sampled at 100 wavelengths across the range 1.45 – 1.65 μm and our retrieval algorithm, NEMESIS (Irwin et al., 2008), used to retrieve continuous profiles of aerosol specific density. This model uses the method of optimal estimation (Rodgers, 2000), but is adapted for use with planetary observations. Scattering is modelled with the Matrix operator plane-parallel method (Plass et al. 1973). Although the assumption of a continuous distribution of aerosols means that thin detached layers are not well captured, the model has the advantage of being extremely simple and robust. The alternative of modelling the spectra with a few thin clouds would require ad hoc decisions to be made concerning the number cloud layers and their pressure levels and would be difficult to automate. In practice we have found that such models provide a very good approximation to the measured

near-infrared spectra of giant planets (Irwin and Dyudina, 2002) and can always be interpreted in terms of equivalent thin layers as required.

Initial test retrievals of spectra near the equator were used to choose an appropriate amount of forward modelling error to tune the retrieval model. It was found that even when using the new k-data of Karkoschka and Tomasko (2009b), we were unable to fit the spectra to within their random error estimates. Although there are several sources of potential error in the model, we attributed this discrepancy to the spectroscopic data, which, although much improved over the data used previously, are extremely difficult to measure under the cold temperatures and long path lengths in Uranus' atmosphere (e.g. Sromovsky et al. 2006, Irwin et al. 2006). To quantify how well we could actually hope to fit these spectra, test retrievals were performed where all vertical smoothing constraints were removed, allowing the retrieval model to fit to the observed spectrum as closely as it could, albeit at the expense of allowing random errors in the measured spectra to propagate through as unrealistic oscillations in the retrieved cloud profile – an effect known as 'ill-conditioning'. The root mean square difference spectrum between the observed and best-fit spectrum was then smoothed to remove higher frequency components and then used as our forward modelling error spectrum, which was added to the observed error spectrum as a simple means of ensuring that the retrieval model did not attempt to fit the measured spectrum to any higher degree of precision. Once this forward modelling error was set, test retrievals were performed with a range of a priori cloud density profile and errors. From these tests we found that using an a priori cloud density profile of $(4.00 \pm 1.75) \times 10^{-5}$ particles/gram of atmosphere at all levels led to the best trade-off between requiring a good fit to the measured spectrum, but also requiring sufficient constraint to prevent unrealistic artefacts appearing in the retrieved cloud profiles. The a priori

value itself of 4.00×10^{-5} particles/gram of atmosphere was chosen to give a reasonable first spectrum, but is actually irrelevant at pressure levels where the measurements contain meaningful information, since the same cloud density is retrieved at these levels regardless of the initial a priori value as was shown by Irwin et al. (2009). The same forward modelling error spectrum was used for all latitudes and for latitudes nearer the limb (which have lower radiance due to mixing with space) this meant that the forward modelling error was a larger fraction of the measured radiance and thus that these measurements were taken to be less reliable, which is entirely realistic since here there are additional errors here in estimating how much mixing with space there actually is.

[Figure 2, Figure 3]

Once tuned, the retrieval model was run on all observations of the 1.45 – 1.65 μm region made in 2006 – 2008. To compare most easily the cloud structures retrieved in each year we present here only retrievals from data recorded under optimal seeing conditions, as discussed by Irwin et al. (2009). These observations had an estimated seeing of 0.48" at wavelengths between 1.4 and 1.6 μm. Unfortunately, although context images were used to monitor the passage of discrete storms across Uranus' central meridian, both the H-band observations of 2007 coincided with the transit of the same storm at 30ºN, which was discussed by Irwin et al. (2009) and can be seen in Fig. 2, which shows contour maps of the retrieved vertical/latitudinal cloud structures for 2006, 2007 and 2008 using the new methane absorption data of Karkoschka and Tomasko (2009b). We again find that: a) the main cloud deck is at slightly lower pressures polewards of 45° N,S; b) the cloud at 45°N thickened from 2006 to 2008; and c) that the contrast between the equatorial zone and darker equatorial belts increased during this time. We found we were able to fit these spectra

with a similar precision to that achieved with the methane absorption data of Irwin et al. (2006), unlike Fry and Sromovsky (2009), who find the fit to be slightly worsened with their model. The differences between the retrieved profiles can best be seen in Fig. 3, which shows the differences from 2006 to 2007, 2007 to 2008, and finally the overall change from 2006 to 2008. The cloud structure retrieved from the 2008 observations with the new k-coefficients of Karkoschka and Tomasko (2009b) is compared with that retrieved using the absorption data of Irwin et al. (2006) in Fig. 4. It can be seen that the overall latitudinal variation is very similar, but the cloud structure retrieved with the new methane absorption coefficients is shifted upwards from 3–4 bars to 2–3 bars and also extends less in depth. It also appears to have greater opacity, but part of this is due to the units used here of optical depth/bar. Since the revised cloud is at lower pressures and spread over a smaller range of pressures we need a higher cloud density to get the same total optical depth. This can be seen more clearly in Fig. 5, where the vertical profiles retrieved at 30°S, equator and 30°N from the 2006 data using the old and new methane absorption data are compared. Figure 6 shows the cumulative optical depth from space down to individual levels calculated for the equatorial retrieved profiles of the 2006 observations using both sets of k-data. Here we can see that with both sets of k-data there is very little optical depth retrieved for stratospheric hazes, consistent with earlier studies (West et al., 1991), However, in the main cloud deck, the integrated opacity increases rapidly. Simplistically one would expect the reflection to come mainly from the region where the vertically integrated optical depth is 0.5 since then the optical depth down to that level and back to space is 1. Reading off the graph it can be seen that the corresponding pressure levels are 2-3 bars for the Karkoschka k-data and 3-4 bars for the Irwin k-data, consistent with the retrieved levels discussed earlier.

[Figure 4, Figure 5, Figure 6]

A concern regarding the reliability of these retrievals is the fact that the deep abundance of methane was set at 1.6% (with a relative humidity above the condensation level of 30%) and assumed not to vary with latitude. As noted earlier and by Irwin et al. (2009), Karkoschka and Tomasko (2009a) have shown from HST STIS observations between 300 and 1000 nm that there is persuasive evidence that the deep methane mole fraction actually increases from 1-2% polewards of 45° to something more like 4% at latitudes between 45°S and 45°N. However, as when using the k-data of Irwin et al. (2006), we found that just increasing the methane abundance (and keeping temperature fixed) did not result in the clouds moving to lower pressures when using the Karkoschka and Tomasko (2009b) data – in other words the suspected latitudinal variation in deep methane abundance has no significant effect on our results if the temperature profile remains fixed. One reason for this is because the methane absorption data of both the Irwin et al. (2006) and Karkoschka and Tomasko (2009b) are a stronger function of pressure than they are of path length. Hence, although the calculated transmission spectrum, using the Karkoschka and Tomasko data, to a deep pressure level (6.3 bars) with a deep methane mole fraction of 1.6% and 4% showed a considerable reduction in transmission over the range 1.45 to 1.75 μm, there was little difference in the spectral shape. However, another reason is due to the choice of temperature profile, which is important when calculating these effects and was not considered in our previous paper. From Voyager 2 radio-occultation measurements Lindal et al. (1987) derived a set of different T/P profiles that varied depending on the assumed methane abundance in order that methane condensed at around 1.5 bar in all cases to account for the sudden change in number density detected by the Voyager 2 radio-occultation experiment at this level. Their 'F' profile,

which assumes a methane mole fraction of 4% is some 8K warmer at pressures below 1.5 bar than the nominal 'D' model as can be seen in Fig. 7. When this T/P profile is used together with a methane mole fraction of 4%, the cloud density profiles shown in Fig. 8 are retrieved. Here the clouds are found to be much higher at just less than 2 bars. It seems unlikely that the temperature profile changes drastically with latitude at pressures greater than 1 bar as the atmosphere is expected to be barotropic at these levels. If we assume that the Lindal 'F' temperature profile is correct at all latitudes at pressures greater than 1 bar and if we assume that methane is more abundant at latitudes less than 45°N,S with a mole fraction of 4% compared with 1.6% at more polar latitudes as estimated by Karkoschka and Tomasko (2009b) (which is also consistent with microwave observations showing more ammonia absorption in the deep atmosphere at these latitudes, Orton et al. 2007; Hofstadter and Butler, 2003) then the pressure level of the main retrieved cloud deck starts to look consistent with being the main methane cloud deck, especially as we would then expect methane clouds to condense at lower pressures at latitudes closer to the poles, which is exactly what is seen in Fig. 8 and also suggested in Fig. 7.

[Figure 7, Figure 8]

Fits to the Long J (1.28 μm) reflectance peak

The processed measured spectra in this peak were again sampled at 100 wavelengths across the range 1.17 – 1.31 μm and NEMESIS used to retrieve the specific density profile of aerosols in exactly the same manner as described in the previous section. The reference T/P and methane profiles were used and we again estimated the forward modelling error by first fitting the spectrum at the equator with minimal constraint and smoothing the difference spectrum. The cloud density a priori error was then again

tuned to give optimal balance between measurement and it was found that the same a priori value and error used in the 1.57 μm fits provided the appropriate level of constraint.

[Figure 9, Figure 10]

Once tuned, the retrieval model was run on the best spatially resolved Long J (1.17 – 1.31 μm) observations made from 2006 to 2008, which had a spatial resolution of 0.48" in 2006 and 2008, and 0.6" in 2007. Figure 9 shows contour maps of the retrieved vertical/latitudinal cloud structures for 2006, 2007 and 2008, and Fig. 10 shows the differences. We found that the fits using the new k-data were slightly improved over those achieved previously with the Irwin et al. (2006) k-data and we find a similar inter-annual variation between the retrievals and similar latitudinal variation. More importantly, however, while Irwin et al. (2009) reported rather different cloud profiles retrieved from the 1.6 and 1.3 μm peaks, the cloud profiles retrieved with the Karkoschka and Tomasko (2009b) data are much more consistent with each other as can be seen in Fig. 11. We will return to this later.

[Figure 11]

Fits to the Short J (1.07 μm) reflectance peak.

The measured spectra in this peak were sampled at 70 wavelengths across the range 1.03 – 1.15 μm and NEMESIS used to retrieve the specific density profile of aerosols. A smaller number of wavelengths was used here both because the wavelength range was smaller than the other two cases and also because the Uranus spectrum has fewer fine features in this peak. We originally found (Irwin et al., 2009) that we were unable to fit the observed spectra at these wavelengths satisfactorily and attributed this to the methane band coefficients of Irwin et al. (2006) not being reliably extrapolated to

Uranus' conditions at these wavelengths. However, we have since come to realise that while this is partly the case, the dominant factor here is that the assumed single scattering albedo of the cloud particles of 0.75 is too small at these shorter wavelengths. Increasing the single scattering albedo to be close to unity we find that we are better able to fit the whole spectrum. We found that using the new k-data of Karkoschka and Tomasko (2009b) provided a substantially better fit to these spectra than the Irwin et al. (2006) k-data, although the fits are still not as good as they are at the longer wave peaks and so are not shown here. However, we find that the main cloud again appears to be located between 2 and 3 bars as it does when retrieved from the Long J and H peaks if we assume the reference T/P and methane mole fraction profiles.

Fits to all the reflectance peaks.

Fits with the methane k-coefficients of Irwin et al. (2006) show considerable inter-band variations, but not so with the Karkoschka and Tomasko (2009b) coefficients, where the retrievals in all three spectral bands (Short J, Long J, H) all basically derive a very thin extended stratospheric haze overlying a cloud at 2-3 bars. This led us to attempt to model simultaneously the entire 1.00-1.75 μm range and try to infer particle scattering properties.

We selected the 2007 observations for this study and extracted the observed Short J, Long J and H-band spectra near the disc centre, but avoiding the rings. Due to some calibration problems of the Short J observations in regions of low reflectivity, the Short J spectrum was replaced with a spectrum measured with the IJ grism during the same 2007 campaign. We compared our spectrum with a reference spectrum of Uranus recorded by the NASA Infrared Telescope Facility (IRTF) SpeX instrument

(Rayner et al., 2009) and found very good correspondence at all wavelengths. Using the cloud structure retrieved from the 1.57 μm window at the disc centre, a synthetic spectrum was calculated from 1 to 1.75 μm, which is compared with the measured spectrum in Fig. 12. The original calculation assumed particles of mean radius 1 μm with a single scattering albedo at all wavelengths of 0.75 and a forward asymmetry of 0.7. The synthetic spectrum naturally matches that measured by the HK grism, but remarkably it also simultaneously provides a very good fit to the Long J peak also. At shorter wavelengths the original calculated spectrum was unable to match the high reflectance seen, but by increasing the single scattering albedo to 1.0 at wavelengths less than 1.2 microns, as has been done in Fig. 12, it can be seen that a reasonably good fit is then achieved over the entire wavelength range. This suggests either that the particles of the main cloud deck are indeed more scattering at this wavelength or that the methane absorption coefficients are erroneously high in the peak.

[Figure 12]

3. Observations of Neptune

During 2007 some observations were also made of Uranus' sister planet, Neptune. Neptune presented a disc of diameter ~2.4" during these observations and thus UKIRT's achievable angular resolution is equivalent to ~1/4 of the disc. However, the observations presented here were made with poorer observing conditions of 0.84", equivalent to only ~1/3 of the disc. Hence, only the broadest latitudinal variations in cloud structure are retrievable from these observations.

UKIRT observations of Neptune were made in all three spectra ranges: Short J (1.1 μm), Long J (1.3 μm) and H (1.6 μm) as detailed in Table 2. Figure 13 presents a combination of the processed grism spectral arrays over the 1.0 – 2.5 μm range,

showing the variation in reflectivity along Neptune's central meridian together with the centre-of-disc spectrum. From Fig. 13 we can see that the southern part of Neptune's disc was considerably brighter than the northern part in 2007, although it is not possible to ascribe this to a hemispheric asymmetry since a large fraction of the northern hemisphere is hidden from view and what we do see, we see at a high emission angle. Figure 13 also compares Neptune's centre of disc spectrum with that observed for Uranus. It can be seen that the peak reflectivities are very similar, but that Neptune has considerably more reflection between the peaks, pointing to the known greater optical depth of hazes in the upper atmosphere of Neptune.

[Figure 13, Table 2]

The Neptune observations were processed in exactly the same way as the Uranus observations and fits were first attempted to the H-band observations and then to a combination of all observations. The H_2-H_2 and H_2-He collision induced absorption coefficients of Borysow (1991, 1992) and Zheng and Borysow (1995) were again used and for simplicity an equilibrium ortho/para H_2-ratio was assumed at all altitudes and latitudes. Although Conrath et al. (1998) concluded that there was some variation in the ortho/para ratio from Voyager 2 thermal infrared observations, the effects in the wavelength bands we considered are very small.

Fits to the H-band (1.57 μm) reflectance peak

The temperature profile we used in this study for Neptune was based on the 'N' profile determined by radio-occultation from Voyager 2 by Lindal (1992) and extended to higher pressures in the troposphere assuming a saturated adiabatic lapse rate. Since the vertical temperature profile again cannot be determined from these observations, the temperature profile was fixed for these retrievals. The deep methane

mole fraction was set to 2.2% (Baines and Hammel, 1994), and followed the saturated vapour pressure curve at pressures less than 2.3 bars until it reached a value of 3.5×10^{-4}, at which it was then fixed at all lower pressures (Baines and Hammel, 1994). The assumed T/P profile and methane mole fraction profile are shown in Fig. 7.

As with the Uranus analysis, an estimate of the forward modelling spectrum was first determined by removing all constraint from the retrieval model and smoothing the resulting difference spectrum. The a priori cloud density profile was then adjusted to $(4.000 \pm 0.875) \times 10^{-4}$ particles/gram of atmosphere where we found that the initial spectrum was reasonably close to that measured and that roughly equal weight was placed on the measurements and on the a priori constraints, resulting in the optimal smoothed cloud profile.

We then attempted to retrieve Neptunian cloud profiles using the same assumptions of particle scattering properties as had been assumed for Uranus, but we found that our fits became increasingly poor towards more southerly latitudes where the opacity of Neptune's thicker stratospheric haze increased. At these latitudes we matched the wings of the main feature, but the central peak was poorly reproduced. We found here that the initial assumed single scattering albedo of 0.75 at all altitudes was inappropriate for these stratospheric hazes in that the opacity required to match the reflectance in regions of strong methane absorption then provided too much absorption for light reflected from the deeper clouds. We thus experimented with different single scattering albedoes and found the fit was best when a single scattering albedo of 0.9-1.0 was assumed. For simplicity we initially assumed a value of 1.0 at all altitudes. The particle asymmetry parameter was left at $g = 0.7$, but we found we could achieve slightly better fits to the 1.57 μm reflectance peak if the particle radius was reduced from 1.0 to 0.5 μm.

Once tuned, the retrieval model was run on the observations of the H-band peak with the HK grism, which had an estimated seeing of 0.84". Again, the 1.57-μm reflectance peak was sampled at 100 wavelengths across the range 1.45 – 1.65 μm and Fig. 14 shows contour maps of the cloud structure retrieved using both the k-data of Irwin et al. (2006) and Karkoschka and Tomasko (2009b). Comparing the two retrievals it can be seen that the retrieved clouds are at very similar altitudes for pressures less than 100 mb, where we expect the Irwin et al. (2006) k-data to be reliable, but that at deeper pressures, the clouds retrieved using the Karkoschka and Tomasko (2009b) k-data are at significantly lower pressures at all latitudes. It is very difficult to retrieve towards the limb with these data, but the stratospheric haze density shows a maximum at 45-50°S and an apparent minimum at 10°S, before then increasing at more northerly latitudes. There is also an indication of increased cloud at the 2-3 bar level at more southerly latitudes, but this latitudinal variation is of borderline reliability.

[Figure 14]

Figure 15 shows the cumulative optical depth from space retrieved at the equator and we can see by comparison with Fig. 6 that the stratospheric hazes on Neptune are very much thicker than for Uranus with an optical depth of ~0.2 at 1.6 μm.

[Figure 15]

Fits to all the reflectance peaks.

Having achieved an acceptable fit at 1.57 μm, we then tested to see how well we could fit the other peaks. The recorded Short J, Long J and H-band spectra near the disc centre were all re-scaled (since the absolute photometric calibration of these

observations was poorly known) to a reference InfraRed Telescope Facility (IRTF) SpeX (Rayner et al. 2009) Neptune spectrum. The cloud structure retrieved from the H-band observation was then used to generate a synthetic spectrum at all wavelengths, which is shown in Fig. 16. Here we find that the same cloud structure again provides a very close fit to both the Long J and H-band peaks, although the particle size at all levels had to be increased to 1.0 μm to prevent the reflectivity of the Long J peak being too high. We were unable to fit the Short J peak, however, which we model as being too faint with these assumptions. Guided by our experience with the Uranus spectra, we remodelled the centre-of-disc spectrum by keeping the stratospheric haze profile fixed at that previously retrieved and with a single scattering albedo of 1, but reset the single scattering albedo to 0.75 at pressures greater than 0.5 bar and then refitted the cloud density at these deeper pressures. The resulting cloud profile provided a similar quality of fit to the spectrum from 1.2 to 1.8 μm, but then allowed us to increase the single scattering albedo of the deeper cloud particles at pressures greater than 0.5 bar and wavelengths less than 1.2 μm to achieve the final fit shown in Fig. 16 (where we also reduced the particle radius of the deeper particles to 0.5 μm), which matches all peaks reasonably well. Hence we conclude, just as we did for Uranus, that either the cloud particles at pressures greater than 1 bar are more scattering at wavelengths less than 1.2 μm than they are above (either due to increased single scattering albedo, reduced forward scattering asymmetry, reduced radius, or a combination of all three) or that the Karkoschka and Tomasko (2009b) k-data (and also Irwin et al., 2006) are again too absorbing in this window. The similarity with the Uranus atmosphere is remarkable in that here too the same cloud structure and small (0.5 – 1 μm) particles can match the entire 1.0-1.75 μm spectrum.

[Figure 16]

The spectrum from 1.75-2.5 μm was also measured here, but we find that the H-band cloud structure is less able to fit this region. However, the reflectance in this region is also dependant on the assumed ortho/para hydrogen ratio and the assumed He/H_2 ratio, which were not considered in this analysis. Gibbard et al. (2003) measured this spectral region with Keck AO observations and found the northern mid-latitude clouds to be higher than those at southern mid-latitudes. Unfortunately the low spatial resolution of our data means that we cannot test these conclusions.

4. Discussion and Conclusions

The new methane k-coefficients of Karkoschka and Tomasko (2009b) have been shown to provide a good fit to the observed UKIRT spectra of Uranus in the Long J (1.3μm) and H (1.57 μm) peaks, where the fit is slightly better than that achieved using the absorption data of Irwin et al. (2006). More importantly, however, the new absorption data lead to very similar vertical cloud structures being retrieved in the two wavelength bands, which both put the main cloud deck at slightly lower pressures (2-3 bars) than estimated by Irwin et al. (2009). In addition, we find that the same cloud structure can reproduce the entire 1-1.75 μm spectrum of Uranus, if the particles are assumed to have a radius if 1 μm at all altitudes and if they are assumed to be more scattering at wavelengths less than 1.2 μm. We have chosen to model this by forcing the cloud particles to have a higher single scattering albedo at wavelengths less than 1.2 μm, but we could equally well have adjusted the asymmetry of the Henyey-Greenstein phase function as we find (Fig. 1) that both parameters have a very similar effect on the synthetic spectra. In addition, we find that the retrieved level of the deep cloud moves to significantly lower pressures if we increase the methane abundance and make the deeper atmosphere warmer by using the 'F' T/P profile of Lindal et al.

(1987). Indeed the inferred pressure level using these assumptions would seem to suggest that the main cloud deck could in fact be composed of methane since it then lies close to the expected condensation level for this gas. Unfortunately it is not possible to discern any spectral evidence of the cloud's composition since the features in the measured absorption spectra of methane ice (Grundy et al. 2002) all coincide with strong methane gas absorption features and are thus not detectable.

For Neptune we again find that we require a deep cloud near 2-3 bars, but a very much thicker overlying stratospheric haze, which has been noted before by, among others, Baines and Hammel (1994). In order not to mask the reflection from the deeper clouds we have a clear indication that these haze particles must be highly scattering and have assumed a single scattering albedo of 1.0 and find they have an optical depth of ~0.2 at 1.6 μm. In addition, just as for Neptune, we find that the deeper cloud particles must be more reflective at wavelengths less than 1.2 μm, if the methane absorption data of Karkoschka and Tomasko (2009b) are assumed to be reliable.

It is very interesting to compare the cloud structure retrieved for Neptune's atmosphere with that retrieved for Uranus' atmosphere (using the same methane coefficients of Karkoschka and Tomasko, 2009b) as is shown in Fig. 17. As can be seen we find that Neptune's atmosphere has a much greater abundance of overlying haze, but at deeper pressures there is a surprising degree of agreement, with the main cloud deck seen to peak at roughly 2 bars. It has long been thought that Neptune might have a higher abundance of methane than Uranus, which would lead to its methane cloud being deeper, assuming that Neptune has a similar deep T/P profile as Uranus at depth. Assuming a deep mole fraction of 2.2% and the Lindal (1992) 'N'

T/P profile, the main methane cloud is expected to condense at around 2 bars, which is very close to where we find the tropospheric cloud in this study.

[Figure 17]

Although the use of the new methane absorption coefficients of Karkoschka and Tomasko (2009b) changes the level of our main retrieved clouds for Uranus, it has little effect on our previously reported conclusions on the latitudinal variations of Uranus' cloud structure, nor on the inter-annual variations. It would thus appear that the atmosphere of Uranus is truly dynamic and has responded rapidly to the change in solar forcing through Uranus northern spring equinox in 2007.

Acknowledgements

We are grateful to the United Kingdom Science and Technology Facilities Council for funding this research and also to our support astronomers, Watson Varricattu (2006) and Andy Adamson (2007, 2008). The United Kingdom Infrared Telescope is operated by the Joint Astronomy Centre on behalf of the Science and Technology Facilities Council of the U.K.

References

Baines, K.H., Hammel, H. 1994. Clouds, hazes, and stratospheric methane abundance in Neptune. Icarus 109, 20-39.

Borysow, A. 1991. Modeling of collision-induced infrared absorption spectra of H_2-H_2 pairs in the fundamental band at temperatures from 20 to 300 K. Icarus 92, 273-279.

Borysow, A. 1992. New model of collision-induced infrared absorption spectra of H_2-He pairs in the 2-2.5 micron range at temperatures from 20 to 300 K - an update. Icarus 96, 169-175.

Brunetto, R., Caniglia, Baratta, G.A., M.E. Palumbo, M.E. 2008. Integrated Near-Infrared Band Strengths of Solid CH_4 and its Mixtures with N_2. Astrophysical Journal 686, 1480.

Conrath, B.J., Gierasch, P.J., E.A. Ustinov, E.A. 1998. Thermal structure and para Hydrogen fraction on the outer planets from Voyager IRIS measurements. Icarus, 135, 501-517.

Fouchet, T., Lellouch, E., Feuchtgruber, H. 2003. The hydrogen ortho-to-para ratio in the stratospheres of the giant planets. Icarus, 161, 127-143.

Fry, P. M., Sromovsky, L. A. 2009. Implications of New Methane Absorption Coefficients on Uranus Vertical Structure Derived from Near-IR Spectra. In: Bull. Am. Astron. Soc. Vol. 41 of AAS/Division for Planetary Sciences Meeting Abstracts. pp. 14.06-+.

Gibbard, S.G., de Pater, I., Roe, H.G., Martin, S., Macintosh, B.A., Max, C.E. 2003. The altitude of Neptune cloud features from high spatial-resolution near-infrared spectra. Icarus, 166, 359–374.

Grundy, W.M., Schmitt, B., Quirico, E. 2002. The Temperature-Dependent Spectrum of Methane Ice I between 0.7 and 5 μm and Opportunities for Near-Infrared Remote Thermometry. Icarus 155, 486 – 496.

Hofstadter, M.D., Butler, B.J. 2003. Seasonal change in the deep atmosphere of Uranus. Icarus 165, 168–180

Irwin, P.G.J., Calcutt, S.B, Taylor, F.W., Weir, A.L. 1996. Calculated *k* distribution coefficients for hydrogen- and self-broadened methane in the range 2000-9500 cm^{-1} from exponential sum fitting to band-modelled spectra, J.G.R., 101, 26,137 - 26,154.

Irwin, P.G.J., Weir, A.L., Smith, S.E., Taylor, F.W., Lambert, A.L., Calcutt, S.B., Cameron-Smith, P.J., Carlson, R.W., Baines, K., Orton, G.S., Drossart, P., Encrenaz, T., Roos-Serote, M. 1998. Cloud structure and atmospheric composition of Jupiter retrieved from Galileo NIMS Real-time spectra, J. Geophys. Res. 103, 23,001 - 23,021.

Irwin, P.G.J., Dyudina, U. 2002. The retrieval of cloud structure maps in the Equatorial region of Jupiter using a principal component analysis of Galileo/NIMS data. Icarus 156. 52 – 63.

Irwin, P.G.J., Sromovsky, L.A., Strong, E.K., Sihra, K., Teanby, N.A., Bowles, N., Calcutt, S.B., Remedios, J.J. 2006. Improved near-infrared methane band models and *k*-distribution parameters from 2000 to 9500 cm^{-1} and implications for interpretation of outer planet spectra. Icarus 181, 309-319.

Irwin, P.G.J., Teanby, N.A., de Kok, R., Fletcher, L.N., Howett, C.J.A., Tsang, C.C.C., Wilson, C.F., Calcutt, S.B., Nixon, C.A., Parrish, P.D. 2008. The NEMESIS planetary atmosphere radiative transfer and retrieval tool, J. Quant. Spectrosc. and Rad. Trans., 109, 1136 – 1150.

Irwin, P.G.J., Teanby, N.A., Davis, G.R. 2009. Vertical cloud structure of Uranus from UKIRT/UIST observations and changes seen during Uranus' Northern Spring Equinox from 2006 to 2008. Icarus 203, 287 – 302.

Karkoschka, E., Tomasko, M. 2009a. The Haze and Methane Distributions on Uranus from HST-STIS Spectroscopy. Icarus 202, 287 – 302.

Karkoschka, E., Tomasko, M. 2009b. Methane Absorption Coefficients for the Jovian Planets and Titan. In: AAS/Division for Planetary Sciences Meeting Abstracts. Vol. 41 of AAS/Division for Planetary Sciences Meeting Abstracts. pp. 10.11-+.

Lindal, G.F., Lyons, J.R., Sweetnam, D.N., Eshleman, V.R., Hinson, D.P. 1987. The atmosphere of Uranus - Results of radio occultation measurements with Voyager 2. J. Geophys. Res., 92, 14987-15001.

Lindal, G.F. 1992. The atmosphere of Neptune: An Analysis of Radio Occultation Data Acquired by Voyager 2. Astron. J. 103, 967 – 982.

Martonchik, J.V., Orton, G.S., Appleby, J.F. 1984. Optical properties of NH_3 ice from the far infrared to the near ultraviolet. Appl. Opt. 23, 541 – 547.

Orton, G.S., Hofstadter, H., Leyrat, C., Encrenaz, T. 2007. Spatially resolved thermal imaging and spectroscopy of Uranus and Neptune. Workshop on planetary atmospheres held November 6-7, 2007 in Greenbelt, Maryland. LPI Contribution No. 1376, 93 – 94.

Plass, G.N., Kattawar, G.W., and F.E. Catchings, F.E. 1973. Matrix operator method of radiative transfer. 1: Rayleigh scattering. Appl. Opt., 12, 314-329.

Rages, K., Pollack, J.B., Tomasko, M.G., Doose, L.R. 1991. Properties of scatterers in the troposphere and lower stratosphere of Uranus based on Voyager imaging data. Icarus 89, 359 – 376.

Rayner, J.T., Cushing, M.C., Vacca, W.D. 2009. The Infrared Telescope Facility (IRTF) Spectral Library: Cool Stars. ApJS, 185, 289 – 432.

Rodgers, C.D. 2000. Inverse Methods for Atmospheric Sounding: Theory and Practice. World Scientific, Singapore.

Satorre, M.A. Domingo, M., Millan, C., Luna, R., Vilaplana, R., Santonja, C. 2008. Density of CH_4, N_2 and CO_2 ices at different temperatures of deposition. Plan Space Sci. 56, 1748–1752.

Sromovsky, L.A., Irwin, P.G.J., Fry, P.M. 2006. Near-IR methane absorption in outer planet atmospheres: Improved models of temperature dependence and implications for Uranus cloud structure. Icarus 182, 577 – 593.

Sromovsky, L. A., Fry, P.M. 2007. Spatially resolved cloud structure on Uranus: Implications of near-IR adaptive optics imaging. Icarus 192, 527 – 557.

West, R., Baines, K., Pollack, J. 1991. Clouds and aerosols in the Uranian atmosphere. In *Uranus* (edited by J. Bergstrahl, E.D. Miner and M.S. Matthews), University of Arizona Press, Tucson, AZ.

Zheng, C., Borysow, A. 1995. Modeling of collision-induced infrared absorption spectra of H2 pairs in the first overtone band at temperatures from 20 to 500 K. Icarus 113, 84-90.

Tables

Table 1. Details of Uranus Long Slit Spectroscopy Observations

Date (yyyymmdd)	Time (UT)	Group ID	Grism	Wavelength Range (μm)	Spectral Resolution λ/Δλ	Integration time	Seeing
20060914	07:29	g85	Short J	1.024 - 1.177	1500	16m	0.48"
20060914	08:31	g151	Long J	1.395 - 2.506	2000	16m	0.48"
20060914	09:04	g192	Short H	1.423 - 1.625	1500	16m	0.48"
20060914	10:07	g253	Long H	1.603 - 1.803	2000	24m	0.6"
20070617	13:31	g616	HK	1.395 - 2.506	500	32m	0.48"
20070726	12:25	g253	Long J	1.395 - 2.506	2000	24m	0.6"
20070728	11:30	g106	Short J	1.024 - 1.177	1500	24m	0.72"
20080715	12:57	g418	Long J	1.395 - 2.506	2000	24m	0.48"
20080715	13:34	g451	HK	1.395 - 2.506	500	32m	0.48"
20080726	12:42	g135	Short J	1.024 - 1.177	1500	24m	0.48"

N.B. 'Seeing' was estimated from the FWHM of the associated standard star observation.

N.B.2. These observations were all taken under photometric conditions.

Table 2. Details of Neptune Long Slit Spectroscopy Observations

Date (yyyymmdd)	Time (UT)	Group ID	Grism	Wavelength Range (μm)	Spectral Resolution λ/Δλ	Integration time	Seeing
20070727	09:44	g231	HK	1.395 - 2.506	500	16m	0.84"
20070729	13:09	g275	Short J	1.024 - 1.177	1500	16m	0.6"
20070729	13:49	g315	Long J	1.395 - 2.506	2000	16m	1.2"

N.B. 'Seeing' was estimated from the FWHM of the associated standard star observation.

Figures

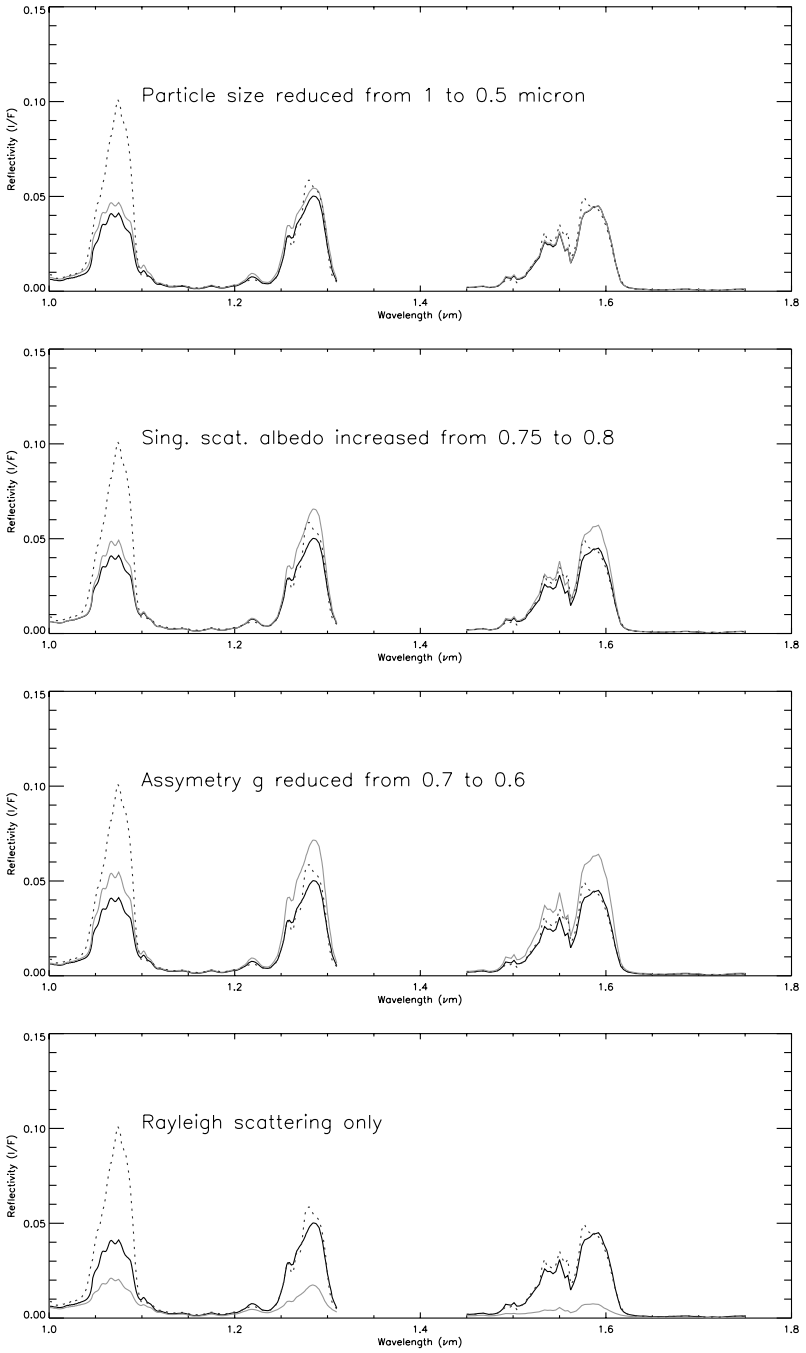

Figure 1. The effect of different scattering assumptions on calculated Uranus spectra. In each of the four plots, the calculated spectrum at Uranus' equator in 2007 deriving from our best fit vertical cloud profile and using the assumed particle properties described in the text is plotted in black, while the measured spectrum is shown by the dotted line. In each plot, the spectrum calculated when one of the scattering

parameters has been modified is plotted in grey. The top plot shows the effect of reducing the assumed particle radius from 1.0 to 0.5 μm. The second plot shows the effect of increasing the assumed particle single scattering albedo from 0.75 to 0.8. The third plot shows the effect of reducing the assumed particle asymmetry factor *g* from 0.7 to 0.6. The fourth plot shows the spectrum calculated when all cloud aerosols are removed and thus scattering is purely from the Rayleigh scattering of the air molecules themselves.

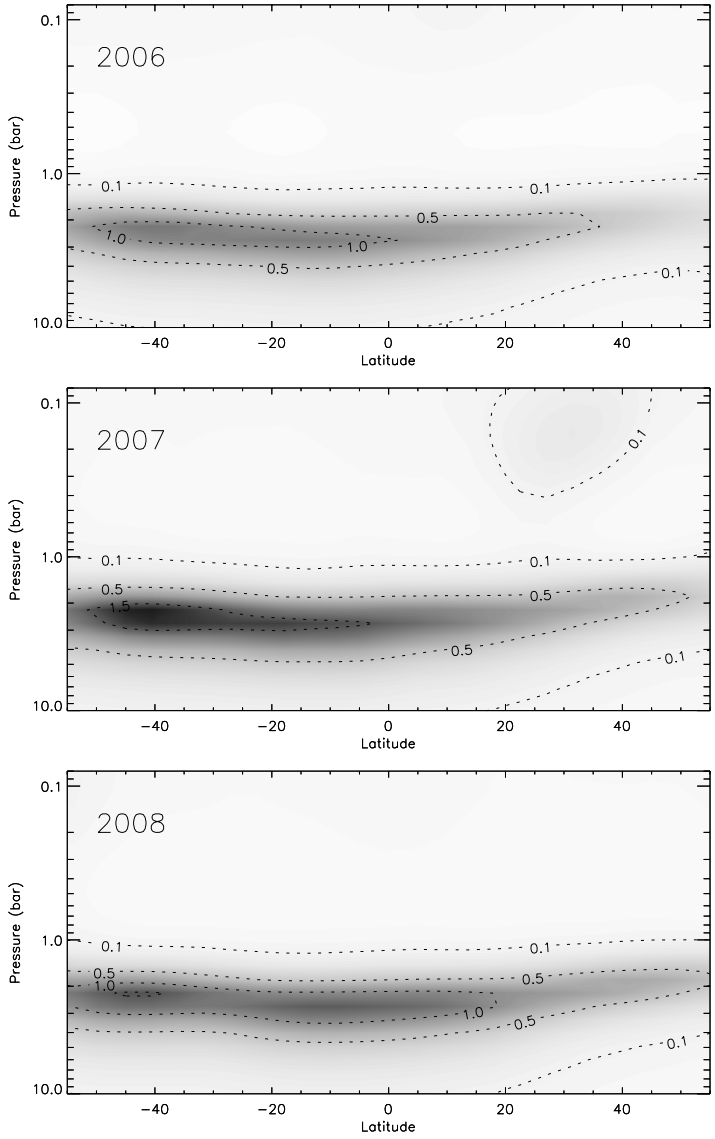

Figure 2. Contour map of retrieved cloud optical depth per bar (at 1.6 μm) profiles, using the new methane absorption coefficient data of Karkoschka and Tomasko (2009b) from fits to the H-band (1.45 - 1.65 μm) spectra at highest available spatial resolution in 2006, 2007 and 2008.

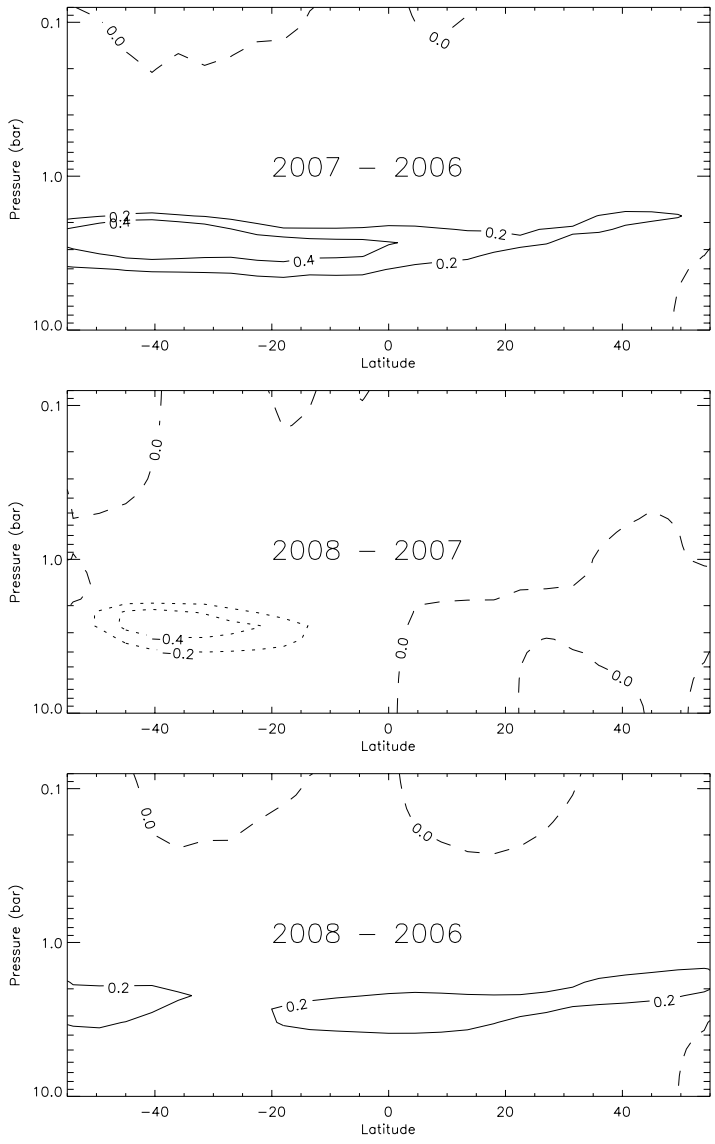

Figure 3. Difference between the retrieved cloud profiles from the H-band (1.45 – 1.65 μm) observations in 2006, 2007 and 2008, shown in Figure 1. Positive differences are indicated by solid contours, negative differences by dotted contours and zero difference by the dashed contour. Top panel shows the change from 2006 to 2007, middle panel shows the change from 2007 to 2008, and bottom panel shows the total change in cloud opacity from 2006 to 2008.

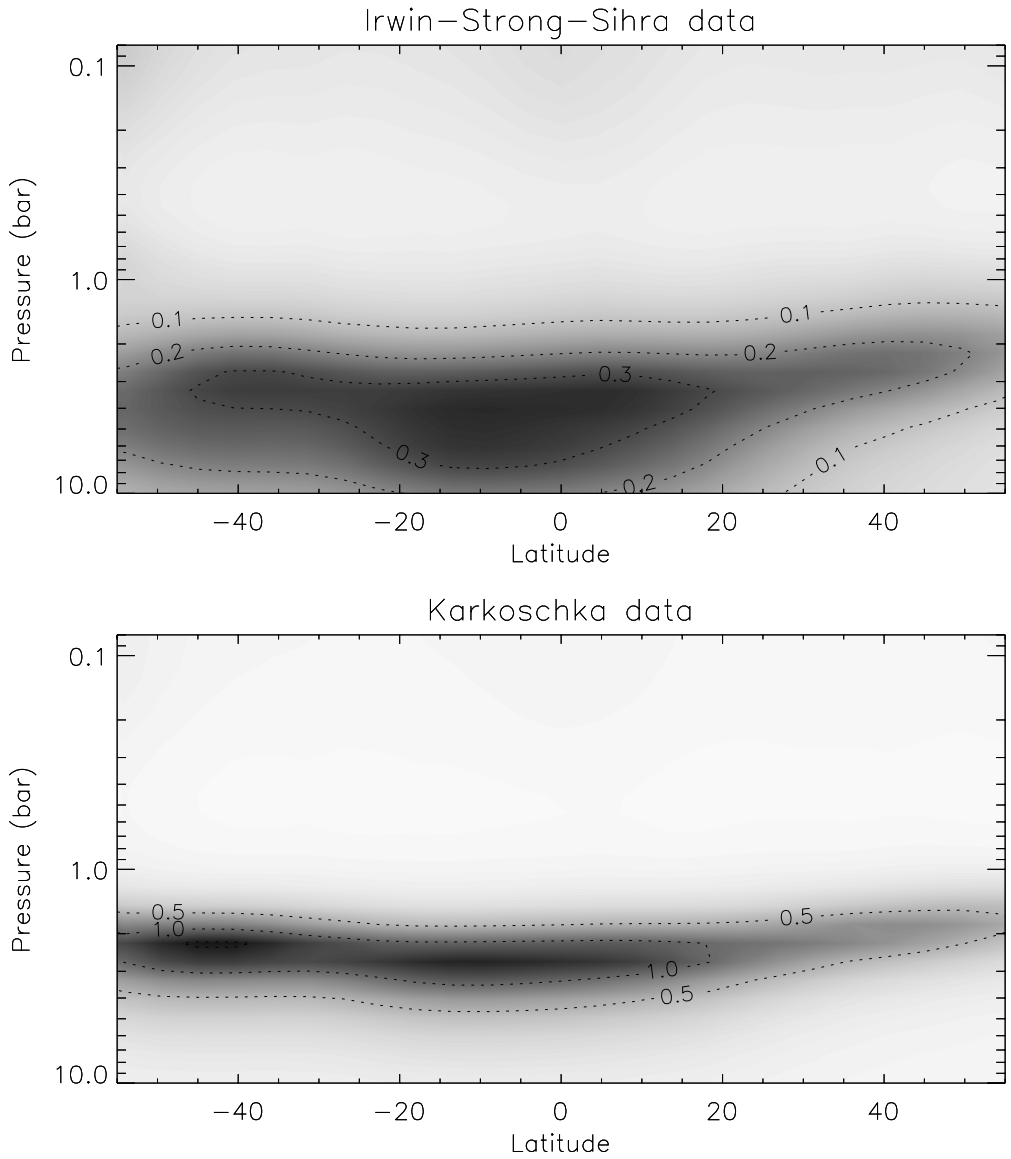

Figure 4. Retrieved vertical-latitudinal cloud structure from H-band observations in 2008 using the k-data of Irwin et al. (2006) and presented by Irwin et al. (2009) (top) and using the new k-coefficient data of Karkoschka and Tomasko (2009b) (bottom).

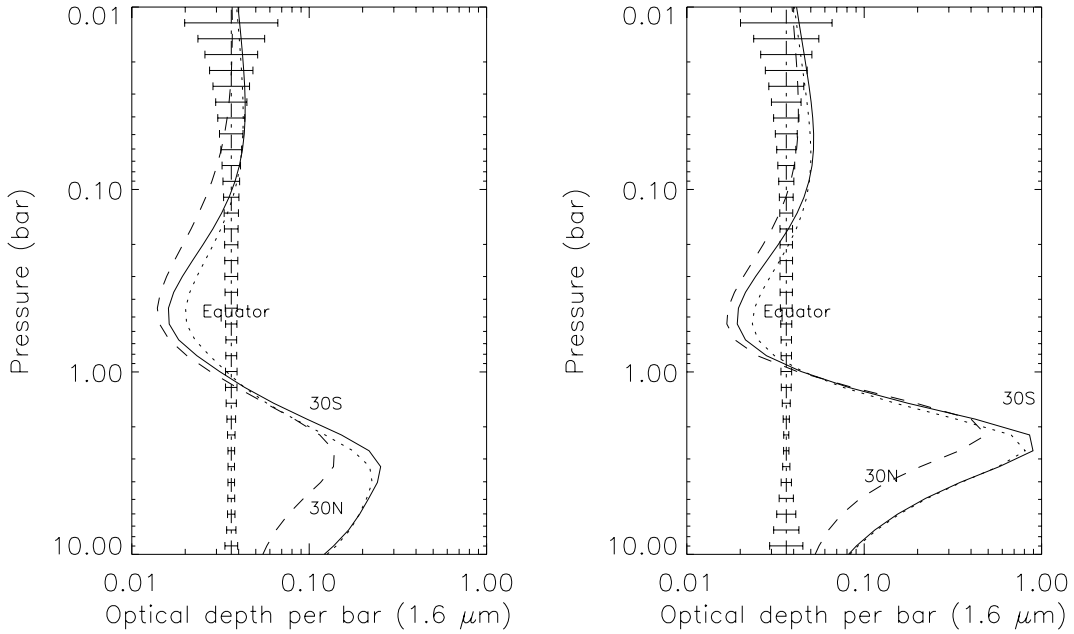

Figure 5. Comparison of vertical cloud structure retrieved from the 1.6 μm peak at 30°S (solid line), equator (dotted line) and 30°N (dashed line) in 2006 using the Irwin et al. (2006) (left) and Karkoschka and Tomasko (2009b) (right) methane absorption data. It can be seen that the Karkoschka and Tomasko (2009b) data put the main cloud deck at lower pressure and make it thicker (in these units of optical depth per bar). The retrieval error bars are indicated for reference about the a priori cloud density profile.

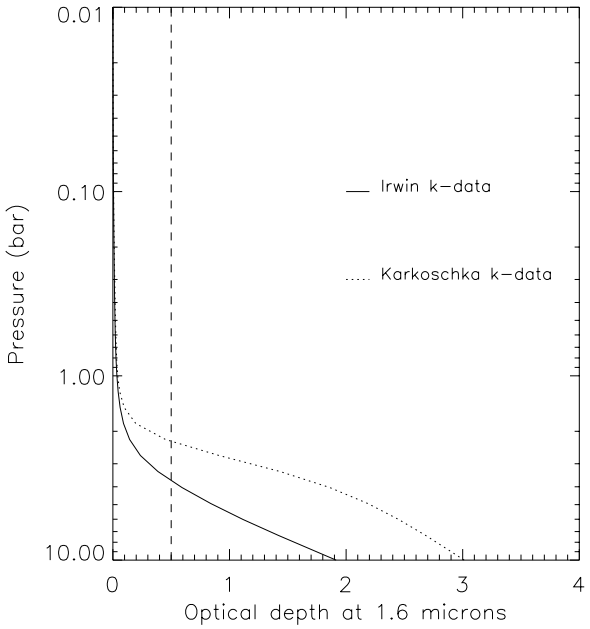

Figure 6. Cumulative optical depth of retrieved clouds at the equator in 2006 retrieved with the methane absorption data of Irwin et al. (1996) and Karkoschka and Tomasko (2009b). The vertical line indicates where the optical depth is 0.5, and thus where the optical depth for a reflecting path is 1.0 and where we expect most of the reflection to come from.

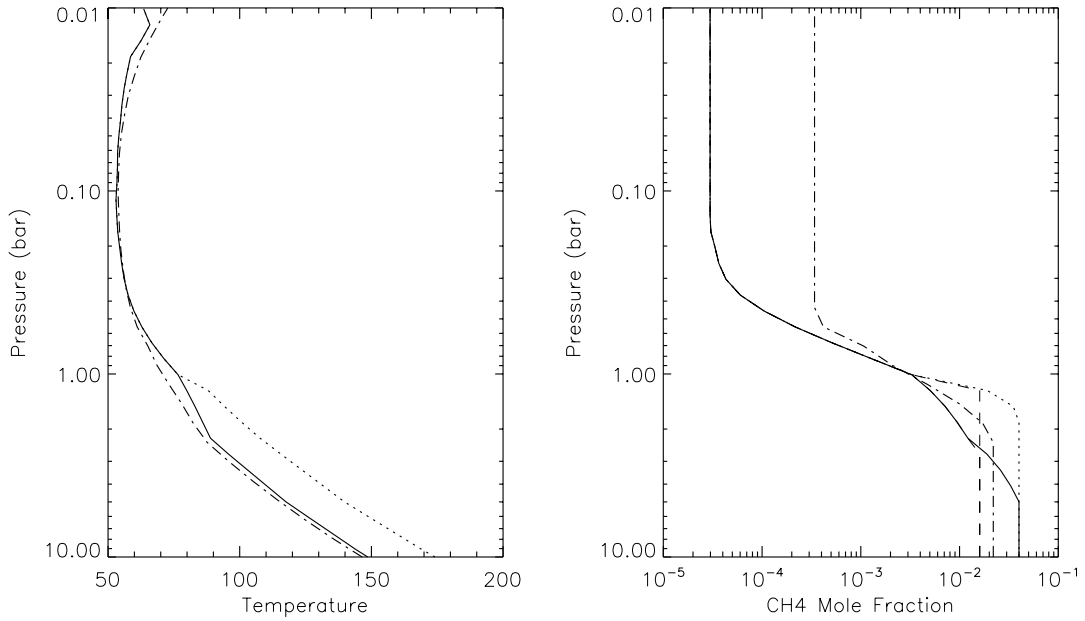

Figure 7. Assumed Uranus temperature/pressure and methane profiles. The left hand panel shows the reference 'D' T/P profile (solid line) compared to the 'F' profile of Lindal et al. (1987) (dotted). The right hand panel shows the resulting methane profile that is obtained after saturation with a deep mole fraction of 4% if the temperature follows the reference T/P profile (solid line) and Lindal 'F' profile (dotted line). The right hand plot also shows the methane profile assuming a deep mole fraction of 1.6% and the Lindal 'F' profile (dashed line). In both panels the dash-dot line shoes the assumed Neptune T/P and methane mole fraction profiles respectively.

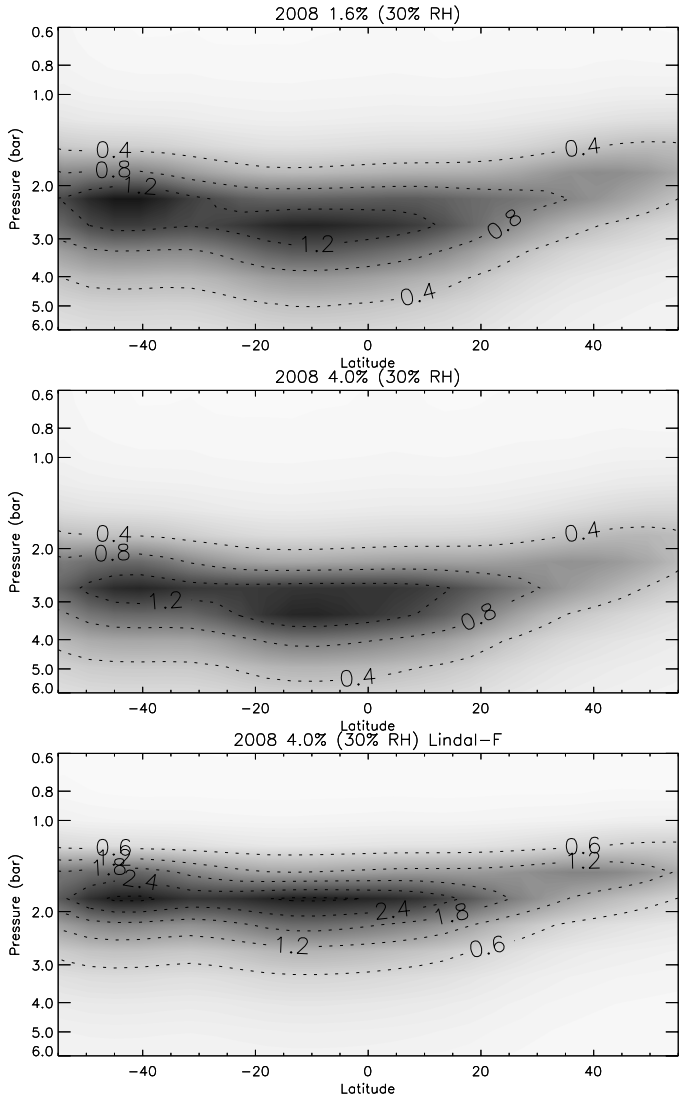

Figure 8. Retrieved cloud structure from the 2008 H-band observations using the Karkoschka and Tomasko (2009b) methane absorption data for different assumptions of the T/P and methane mole fraction profiles. The top plot shows the reference case with the reference T/P profile, deep methane mole fraction of 1.6% and 30% relative humidity above the condensation level. The middle plot shows the retrieved cloud structure when the deep methane mole fraction is increased to 4%, keeping the T/P profile fixed. Here we can see there is very little change in the retrieved cloud structure since the methane abundance in the 1-4 bar region is virtually unchanged (as

can be seen in Fig. 7). The bottom plot shows the retrieved cloud structure when the deep methane mole fraction is set to 4%, but using the warmer Lindal 'F' T-profile. Here the abundance of methane in the 1-4 bar region is greatly increased (Fig. 7) and thus the retrieved cloud decks move significantly upwards.

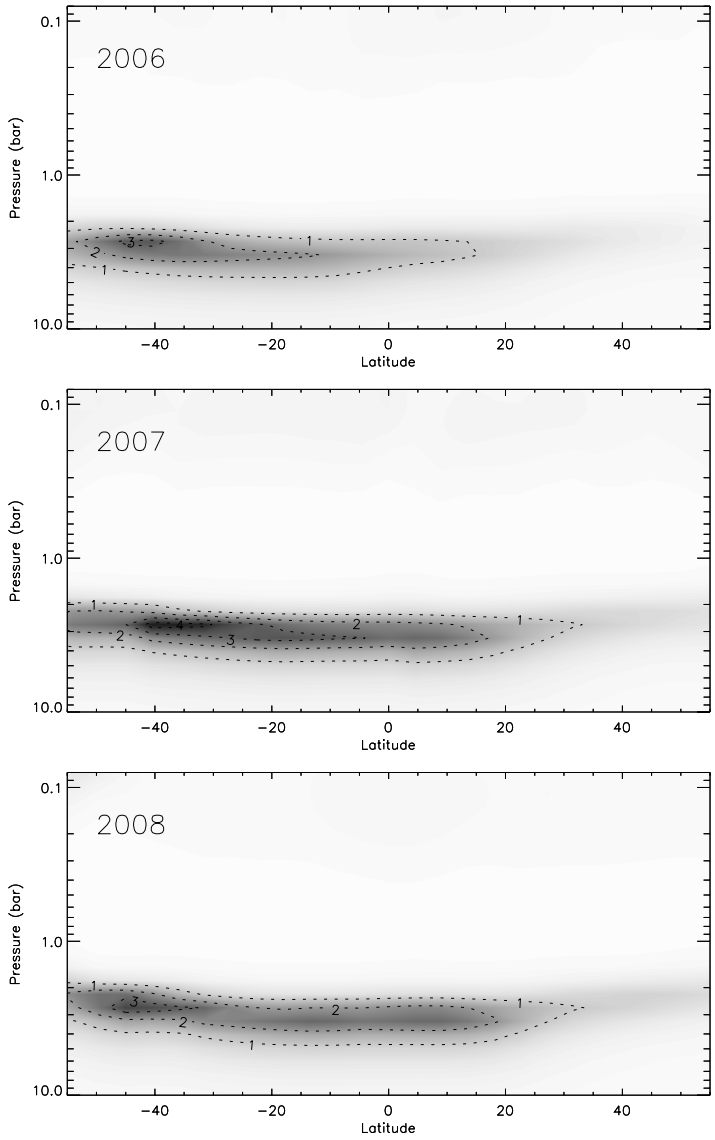

Figure 9. Retrieved clouds contour maps in 2006, 2007 and 2008 from Long J observations using Karkoschka and Tomasko (2009b) methane absorption data. The similarity of the inferred pressure level of the main cloud deck with the H-band retrievals in Fig. 2 is striking.

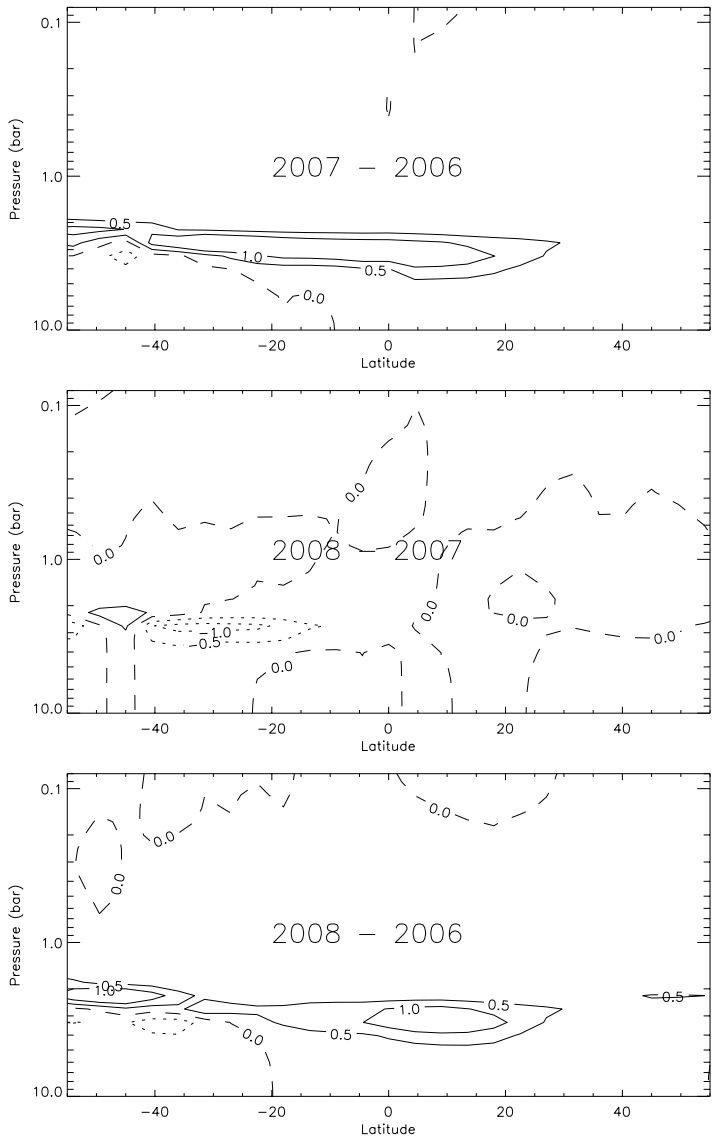

Figure 10. Differences between cloud profiles retrieved from Long J observations in 2006, 2007 and 2008.

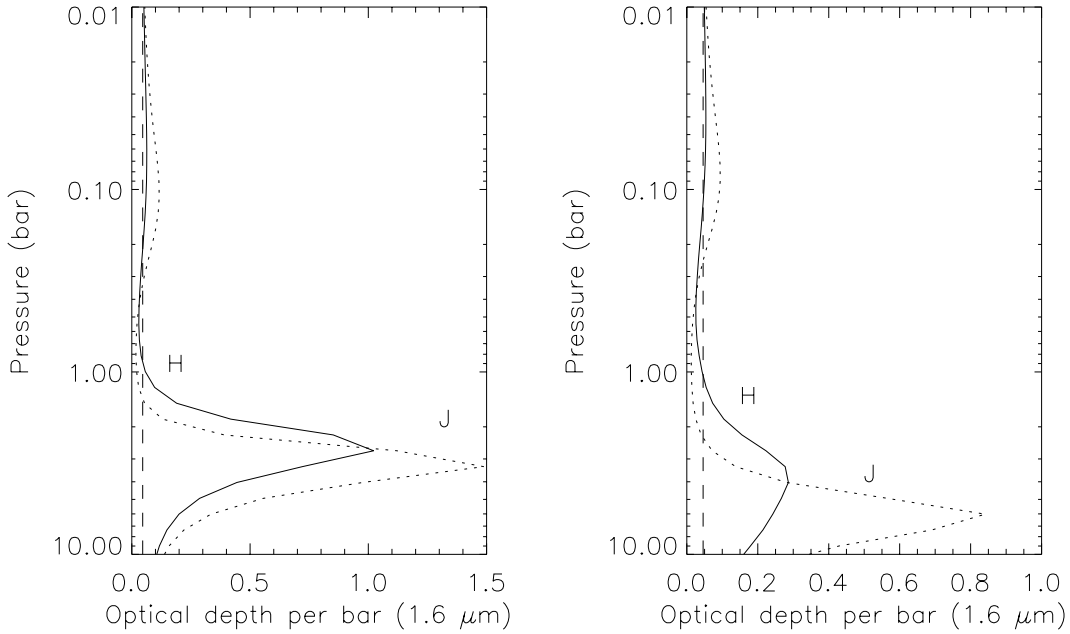

Figure 11. Comparison of H-band (1.6 μm) and Long J (1.3 μm) retrieved cloud optical depth profiles at Uranus' equator in 2006, using the Karkoschka and Tomasko (2009b) methane data (left). The a priori value is indicated by the dashed line and the retrieved profiles can be seen to relax back towards this value at altitudes where the measurements provide little constraint ($p > 8$ bars, $p < 0.08$ bar). The improved agreement between the inferred pressure levels of the main cloud in the two wavelength bands when the Karkoschka and Tomasko data are used is significant when compared to the profiles retrieved using the Irwin et al. (2006) methane k-data (right), previously presented as Fig. 20 of Irwin et al. (2009).

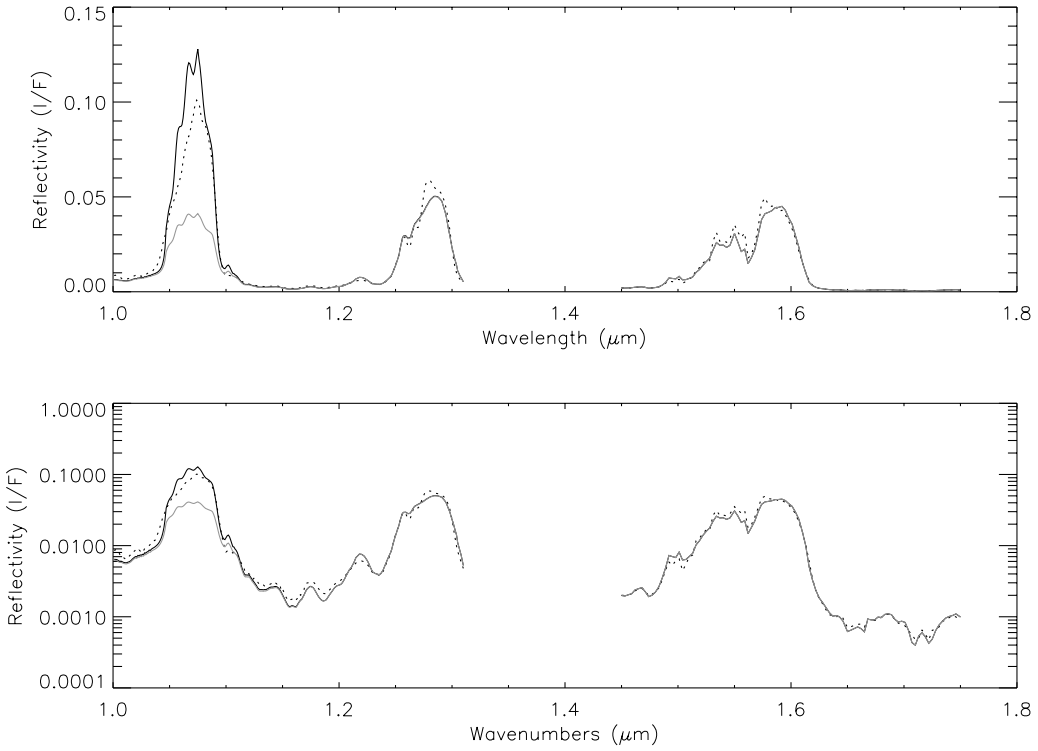

Figure 12. Measured UKIRT observations just south of the Equator (avoiding ring) in 2007 (dotted line) and fit (solid line). Synthetic spectra were calculated from 1 to 1.75 μm from the cloud structure retrieved from H-band (1.45 – 1.65 μm) observations assuming particles of radius 1 μm and single scattering albedo 0.75 at all wavelengths. The simultaneous fit to the peak at 1.3 μm is remarkably good. The 1.07 μm peak was not well fitted originally (light grey line) and the fit shown here could only be achieved by increasing the single scattering albedo of the cloud particles to 1.0 at wavelengths less than 1.2 μm. This suggests either that the cloud particles are indeed more scattering at this wavelength or that the methane absorption is erroneously high in the peak.

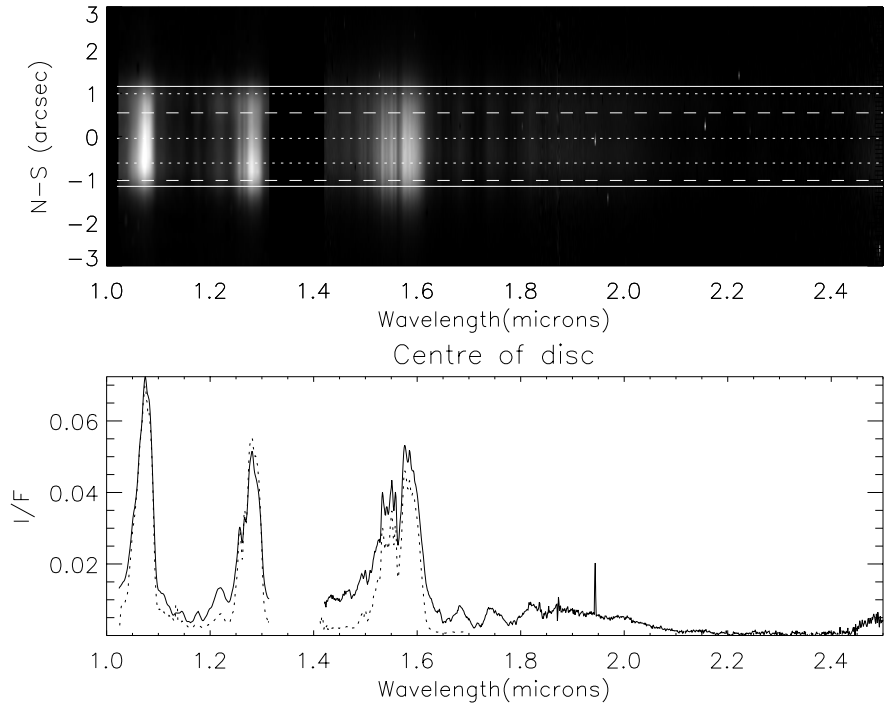

Figure 13. Combined measured spectra across Neptune's disc in 2007 from 1 to 2.5 μm. The top panel shows a spectral image of Neptune where the horizontal axis is the wavelength and the vertical axis is position along the entrance slit, aligned along Neptune's central meridian. The edge of the planet is indicated by the horizontal white lines, the equator and south pole are indicated by horizontal dashed white lines, and latitudes 30°N,S and 60°S are indicated by the horizontal dotted white lines. Three main observable peaks are seen at 1.07, 1.28 and 1.57 μm. The bottom plot shows a cross section (solid line) through the centre of the disc (28ºS) compared with the centre of disc reflectivity of Uranus (dotted line) measured during the same programme.

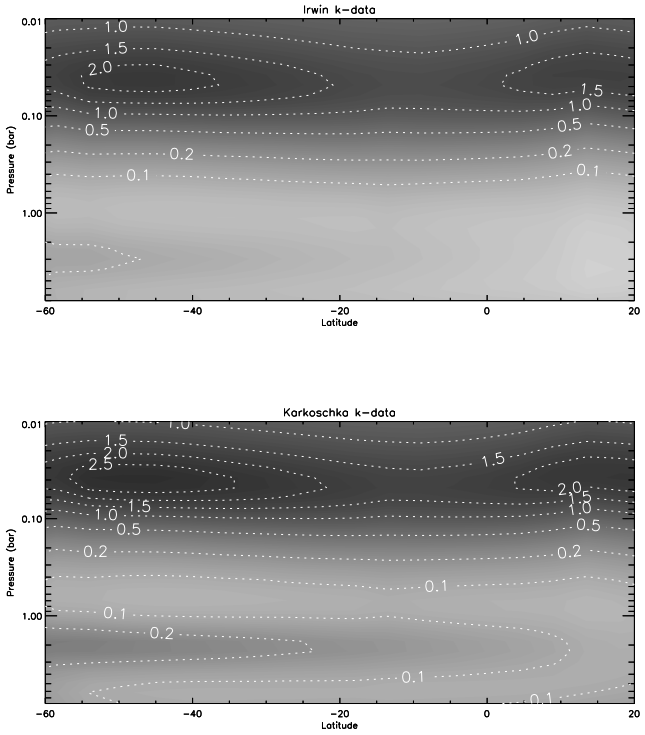

Figure 14. Contour map of retrieved cloud optical depth per bar (1.6 μm) profiles from the fit to the H-band observations. The top panel shows the fit using the k-data of Irwin et al. (2006), while the bottom panel shows the fit using the revised k-data of Karkoschka and Tomasko (2009b). It can be seen that both k-data sets reveal similar latitudinal variations in cloud opacity, but that the deep cloud is more nearly centred at ~2 bars when retrieved with Karkoschka and Tomasko's k-data.

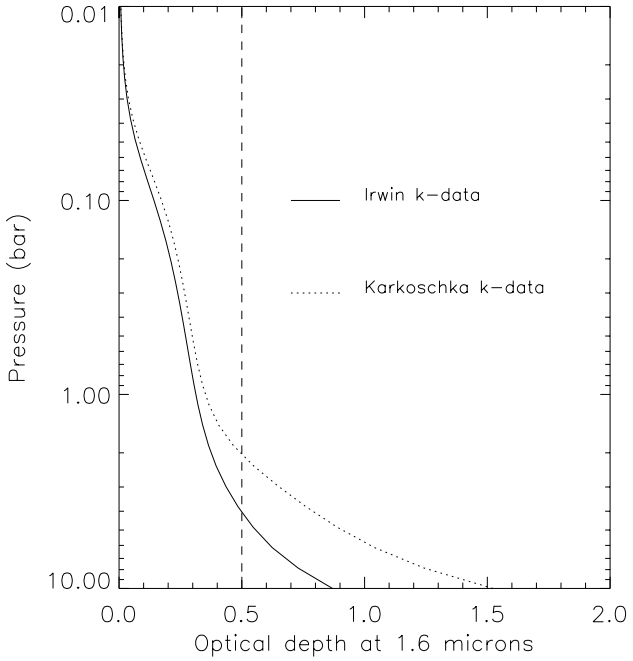

Figure 15. Cumulative optical depth of retrieved Neptunian clouds at the equator in 2007 retrieved with the methane absorption data of Irwin et al. (1996) and Karkoschka and Tomasko (2009b). The vertical line again indicates where the optical depth is 0.5. The increased opacity of stratospheric hazed relative to Uranus (Fig. 6) is clear, and has an optical depth (at 1.6 μm) of approximately 0.2.

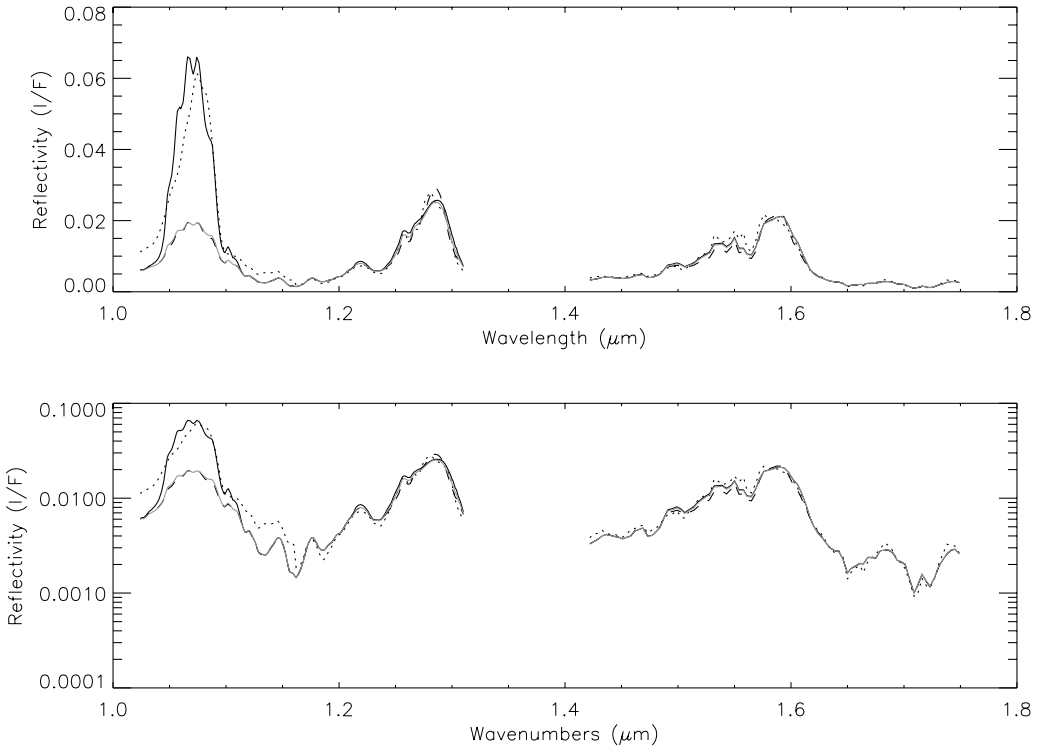

Figure 16. Measured spectra from Short J, Long J and HK grisms (dotted line) near the centre of Neptune's disc, scaled to match the IRTF Neptune reference spectrum (Rayner et al. 2009) at the reflectance peaks. The top plot uses a linear radiance scale, while the bottom uses a log scale. The dashed line shows the synthetic spectrum generated from the cloud structure fitted at 1.6 μm presented earlier. The grey line shows the synthetic spectrum generated from the cloud structure retrieved from the 1.6 μm peak when the haze densities were fixed at their previously retrieved values above the 0.5 bar level (and the single scattering albedo kept at 1.0), but the density of aerosols at lower altitudes, of reduced single scattering albedo 0.75 was allowed to vary. This provides exactly the same quality of fit as before in the H-band, but allows us to then see the effect of increasing the single scattering albedo of the deeper aerosols from 0.75 to 1.0 at wavelengths less than 1.2 μm. The calculated spectrum from this cloud model, where the particle radius of the deeper clouds was also reduced to 0.5 is shown as the solid line and can be seen to provide a reasonably close fit at all

wavelengths. The mismatch near 1.15 μm is due to a calibration problem with the Short J grism observation.

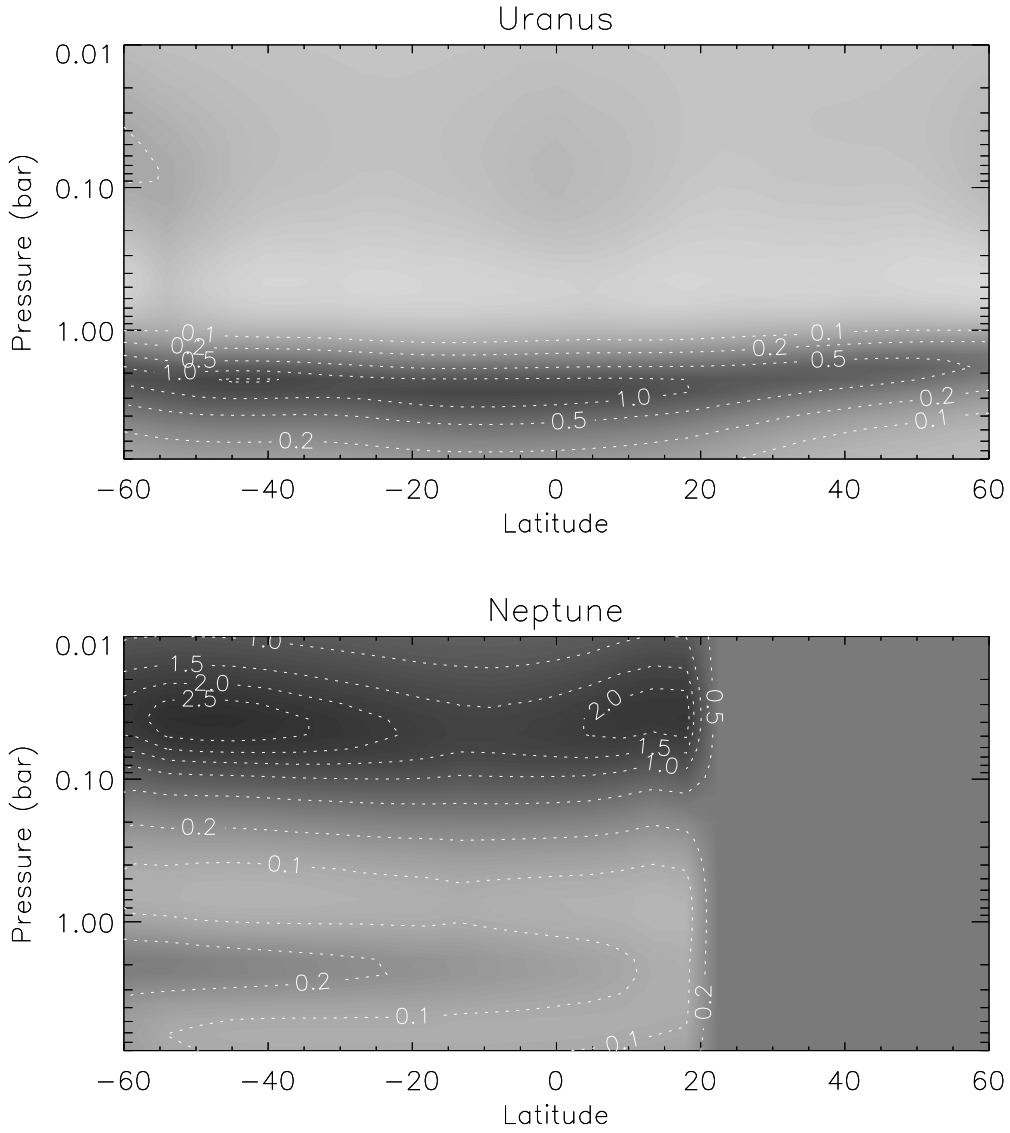

Figure 17. Comparison of the retrieved cloud structures for Uranus and Neptune using the methane absorption of Karkoschka and Tomasko (2009b). Uranus clouds are those retrieved in 2008 from H-band observations. A similar tropospheric cloud is seen for both planets with a peak in opacity at roughly 2 bars. In the stratosphere, the planets differ greatly, with Neptune seen to have the expected much higher abundance of highly scattering stratospheric haze.